Multifunctional concrete with Graphene-based Nanomaterials and Super Absorbent Polymer

Tanvir Qureshi[1]*, Shreyas Ootim[2]

[1]Senior Lecturer, Department of Geography & Environmental Management, University of the West of England, Coldharbour Lane, Frenchay, Bristol, BS16 1QY, UK. Email: tanvir.qureshi@uwe.ac.uk

[2]MSc Civil Engineering Student, Department of Geography & Environmental Management, University of the West of England, Coldharbour Lane, Frenchay, Bristol, BS16 1QY, UK. Email: shreyas2.ootim@live.uwe.ac.uk

* Corresponding author: Tanvir Qureshi

Abstract

This study reports on the development of a multifunctional concrete using graphene nanoplatelet (GnP) and sodium polyacrylate (SP) super absorbent polymer. A combination of concrete functionalities was convened to improve, i.e., high strength and durability along with smart properties such as self-healing and self-sensing. GnP (0.05 wt% of cement) and SP (0.11 wt% of cement) were dispersed in concrete. Compared to the control concrete mix (no GnP and SP), the compressive strength increased 14% by GnP and decreased 9% by SP, and their combination resulted in a 6% enhancement in strength. The durability performance of concrete samples under coupled degradation mechanisms of freeze-thaw and chloride ion ingress suggested that SP in concrete has a better performance than GnP in concrete. SP in concrete shows self-sealing abilities resulting in less chloride ion penetration. However, the combined effect of both GnP and SP in concrete resulted in the maximum reduction in chloride ion penetration depth under freeze-thaw, a 42% reduction compared to the control mix. Microstructural analysis was conducted and found to resist the effects of freeze-thaw and reduce chloride ion penetration in modified concrete compared to the control concrete mix. GnP developed self-sensing abilities in concrete, resulting in about 12.7% fractional change of electrical resistance under 10 KN of cyclic compressive loading. The synergic impact of GnP and SP possesses a new prospect for developing highly efficient multifunctional concrete.

Keywords

Multifunctional concrete, mechanical properties, durability, self-healing, self-sensing.

1. Introduction

Concrete is a ubiquitous material comprised of cement, sand, water, coarse and fine aggregates. This creates a material of high compressive strength and durability yet weak in tensile strength and requires the reinforcement of steel bars to bear tensile stress. Concrete occasionally fails to satisfy engineering requirements due to the inherent brittleness, low tensile strength, high probability of cracking and durability issues (Long et al., 2018). Out of all, the durability performance of concrete is often compromised when exposed to aggressive environments with prominent physical and chemical attacks. The loss of durability further leads to a decrease in structures' service life, increasing environmental burdens and economic costs from maintenance (Long et al., 2019). There is also desire for concrete to be stronger and to have smart properties. Therefore, concrete needs to be multifunctional with enhancement in properties and additional performance required for the future built resilient infrastructure.

Researchers have tried to improve the mechanical properties of concrete by using different types of fibres and additives. The idea of embedding nanotechnology within the concrete would enhance its mechanical properties by controlling nanoscale crack formation has received widespread attention.

A review from Olafusi et al. (2019) stated that nanotechnology is the understanding, examining, controlling through monitoring, and restructuring of the behaviour and performance of materials at the nanoscale between 1 and 100 nanometres to produce a material with fundamentally new properties and functions. Modifying concrete with the addition of nanotechnology is likely to have multifunctional property changes. Table 1 presents theoretical assumptions that can be made from the inclusion of Nanotechnology in Concrete. Nanomodification of concrete could upgrade properties such as increase in strength, ductility, electrical conductivity, durability performance, thin coating of reinforcement in concrete exposed to harsh environment, develop self-sensing abilities, thin structural elements and adjoin sustainability.

Nano science and technology facilitates a bottom-up approach to impact the properties of cement-based composite. The concept of nano-engineered cementitious composites is based on nano-core effect which is dictated by nano-core-shell element (Han etal., 2019). In that context, graphene and its derivative 2D nanomaterials have much attention for improving the cement-based composite properties to make it multifunctional.

1.1. Graphene derivatives and their impact on concrete

2D-Graphene was first isolated in Manchester in 2004 by Professors Andre Gein and Kostya Novoselov through a simple method of using sticky tape to remove flake layers by layer from a lump of bulk graphite. Through constant graphite fragment separations, flakes of graphene, one atom thick were created. Graphene-based materials can be classified according to their thickness, lateral size, and functionalisation state (carbon to oxygen atomic ratio) (Qureshi and Panesar (2019), Qureshi and Panesar (2020) and Qureshi et al. (2019)). Graphene-based materials are commonly classified as pristine graphene (monolayer), few layers of graphene (2 to 10 layers), functionalised graphene (graphene oxide (GO), and reduced graphene oxide (rGO)), graphene nanoplatelet (GnP) (10 to 70 layers).

GnPs, among other derivatives of graphene, exhibit fascinating properties. GnPs have a planer structure, thus allowing it to have the ability to transfer the stress to other positions and relieve the stress concentration in the matrix (Wang, Jiang and Wu, 2016). It is lightweight, display mechanical toughness, are low in cost production, has thermal conductivity and poses electrical conductivity properties. Due to their 2D flat morphology with electrical conductivity properties, GnPs can be used as a nano inclusion for developing piezo resistivity properties in the different composite systems (Tao et al., 2019 and Sun et al., 2017). These properties indicate that GnPs are an attractive option that can be used within the concrete industry compared to other Graphene derivatives.

Graphene is known to be hydrophobic, making it challenging to disperse in water for mixing in concrete. Du and Pang (2018) investigated the effectiveness of dispersing GnP in water and identified key challenges, such as aggregation in polar solvents. Dispersion of the nanoparticles is also challenging in a high pH solution and mix such as cement paste (Qureshi and Panesar, 2017). The dispersion challenge of GnP and other graphene derivative were commonly tackled using surfactants which can keep the 2D sheets separated to remain suspended rather than flocculated, as well as using ultrasonication and high share mixing (Qureshi, Peterson, Panesar, 2019). Often a combination of those approaches has been noted in the literature.

An appropriate proportion of GnPs is required combining with cement in a controlled design mixture of concrete to enhance the desirable performance of concrete. In addition, proper dispersion of GnPs is required to attain full realisation of the performance improvements in concrete. A small dosage of GnP (0.02 wt% of cement) in cement paste composite was reported to enhance the 28-day compressive and flexural strength by 39% and 38%, respectively, compared to the control mix with plane cement paste (Qureshi and Panesar, 2020). Then again, in a more complex cement based composite system such as in mortar and concrete, Wang, Jiang, and Wu (2016) reported that adding 0.05 wt% GnP in cement resulted in 15–24% and 3–8% increases in the flexural and compressive strengths. Another report by Tao et al. (2019), stated that the maximum values were attained when 0.05 wt% GnP was used. The compressive and flexural strengths increased from 49.5 MPa and 7.7 MPa to 53.6 MPa (by 8.3%) and 8.9 MPa (by 15.6%). Chen et al. (2021) observed that "when the GnPs content is 0.04wt%, the flexural and compressive strength of cement mortar can still be increased by 12.8% and 33.9% after 28 d". However, incorporating an excessive amount of GnP beyond 0.04% could start to have negative implications such as higher porosity which induces percolations and decreases compressive and flexural strength, as found in their experiment.

The freeze-thaw resistance of graphene cement-based systems has been investigated by researchers. Mohammed et al., (2016) experimented with the freeze-thaw resistance of Graphene Oxide (GO) in mortar. The mechanism of how GO enhances freeze-thaw resistance can be explained by but is not limited to the amount of entrained air due to GO addition, enhancing pore structure, and increasing compressive strength. Chen et al. (2019) investigated the effects of GnP on the freeze-thaw performance of concrete. They concluded that using 0.05 wt% of GnP had an increase of 22.40% in compressive strength, and less mass loss during 200 freeze-thaw cycles (showing the ability to keep the matrices together due to a smaller size range which could refine the internal pore structure) and reduced workability during slump test. Furthermore, GnP caused lower porosity and formed a compact microstructure indicating less water absorption when compared to the control mixture. This is an ideal multifunctional composite developing prospect combining all performances.

Following the aforementioned effects of GnP in concrete, another potentially enhancing property is the self-sensing capabilities within concrete. Tao et al. (2019) identified that GO is relatively electric insulating due to the presence of oxygen-containing functional groups on its surface. However, GnP shows high electric conductance, which in effect tunes the electric properties of concrete more frequently. Qureshi and Panesar (2020) monitored the electrical resistivity of few layer graphene (G), GO and rGO after 24 hours of casting to 28 days. They concluded that the electrical resistivity gradually increases with the hydration times of the mixes. For example, low concentrations of G and GO between 0.01-0.02% were found to have approximately 13% higher electrical resistance after 28 days.

The addition of 2 vol.% multi-layer graphene, a specific grade GnP like materials (1-5 nm thickness and <2 μm diameter), in cement can achieve an enhancement of 54% in compressive strength and 21% in flexural strength to cementitious composites, respectively (Han et al., 2017). Similar grades of graphene derivatives (donated as nano graphite platelets (NGPs)) in a separate study show piezoresistive characteristics to cementitious composites. As an indicator of sensitivity response, fractional change in electrical resistivity of graphene-cement composite with 4 vol%–10 vol% of NGPs can reach 6.7% to 15.6% when the compressive stress is raised up to 20 MPa . The is owing to the high electrical conductivity property of GnP like materials (Sun et al., 2017).

The conductive channels of graphene in cement-based composite develops piezoresistive properties, which can change the material electrical resistivity with its strain (Songmei, Qureshi and Wang, 2021). Le, Du and Pang (2014) investigated the electrical potential method for structural health assessment of cement composites. They found that the mortar reaches high electrical conductivity by adding between 1.2-2.4% of GnP, for 5-10% mass content of cement. Dong et al. (2019) describe a piezoresistive cement-based sensor as a composite material, consisting of a conductive phase (2D-

Graphene Nanoplatelets (GnP), graphite, carbon nanotubes (CNT) or other metallic alloys) distributed in a matrix of a non-conductive phase typically cement paste, mortar, or concrete. This piezoresistivity can be useful for providing structural health monitoring and damage assessment of reinforced concrete structures to maintain the integrity of the structure in the long run as cracks may be detected and fixed at an earlier stage.

1.2. Superabsorbent polymers (SAP)

Super Absorbent Polymer (SAP) is an organic macromolecule substance newly used as an internal curing agent in concrete. SAP contains carboxyl (–COOH), hydroxyl (–OH), and strong hydrophilic groups, which lead to the gelatinous texture once water is absorbed and has a three-dimensional crosslink network structure (Ding, Zhang, and Zhang, 2017). One of the popular SAP is sodium polyacrylate (SP), a polyacrylic acid sodium salt with the chemical formula $[CH_2{-}CH\ (CO_2Na)\ {-}]_n$ and widely used in consumer products such as baby diapers. Since SAP has hydrophilic groups, they form hydrogen bonds with water molecules, thus promoting hydration and proficiency in absorbing large volumes of water (200 to 300 times its original weight) (Anandkumar, Suriya, and Ravichandran, 2020).

Al-Nasra's (2013) work looked into optimising the amount of SP required for concrete to achieve maximum strength and their influence on durability performance. It was concluded that the effective optimum amount of SAP required is 0.11% of cement by weight. Furthermore, Al-Nasra identified that mixing the SP in dry cement first as opposed to water allowed for better dispersion. However, these experiments were conducted with mortar samples, and the effects of SP within concrete samples are yet to be explored comprehensively.

Many experiments have been conducted to identify the strength change of SP in concrete and mortar. Lee et al. (2014) cast SP into a mortar mix and found that there was a 31% improvement in strength compared to plain mortar. However, the flow properties of mortar decreased with the increase in SP volume. Mazur (2015) observed an 18% increase in compressive strength, a 70% reduction in water permeability and 17% less chloride permeability when SP was combined into a mortar mix. Kevern and Farney (2012) found that 33% higher compressive strength and 35% less water permeability can be achieved by adding SP within concrete. Anandkumar et al. (2020) found that the compressive strength of their SP concrete increased from 25.10N/mm^2 to 27.90N/mm^2 after 28 days. The data provided corroborates the reduction of water/chloride ion penetration due to an increase in concrete strength with SP as time proceeds.

Daoud and Al-Nasra (2014) found that Super Absorbent Polymer in a concrete mixture (SAP-Concrete) availed in freeze-thawing cycles, thus proving to act as frost protection. On a microscale level, it can be observed that during hydration, as the SAP slowly releases the water from within (internal curing) it shrinks, leaving greater voids similar to voids created by adding air entrainment agent to the concrete. The air bubbles entrapped in the concrete absorb the hydraulic pressure due to the water freezing. Once frozen, water expands approximately 10% in volume generating hydraulic pressure in the concrete that has the potential to cause the concrete to crack. However, providing voids in the concrete absorbs the hydraulic pressure, reducing susceptibility to freeze and thaw cycles, providing additional space for the water to expand, and improving the workability and consistency.

SP can internally cure the concrete from within as it slowly releases water over time. This is crucial as it mitigates autogenous shrinkage of concrete which causes cracking in the plastic and hardening stage, which could affect the strength and durability of concrete Jensen (2013). Jensen and Hensen (2001) conducted tests to demonstrate that shrinkage reduction due to SP is related to a corresponding increase in the internal relative humidity of the cement paste. They concluded that SAP has the potential to save energy by improving the concrete insulation property and showed that increasing the quantity of SP in the concrete mix increases the insulation degree of the hardened concrete.

Snoeck et al. (2012) investigated the potential of SP possessing sealing/healing capabilities in concrete and reported that treatment or manual repair is required as the low tensile strength causes cracks and invites harmful chemicals into the cracks that damage the durability of concrete. In one test, they swelled SP in concrete after exposing it to a humid environment. A water permeability test and visualisation of permeability tests by neutron radiography were conducted and showed that SP's desorption triggers healing in the cracks. Cracks up to 130μm were able to close completely in wet/dry cycles due to the precipitation of calcium carbonate, and a decrease in permeability was noticed.

1.3. Combination of GnP and SP in concrete

The literature review corroborated that the optimum dispersion of GnP and SP individually in concrete improves its properties. Working individually proposes high-performance concrete. However, when expected to enhance specific properties, GnP and SP composition in concrete pose individual challenges. For the first time, this study investigates the influence of combining GnP and SP in concrete. The hypothesis behind this combination is to achieve multifunctionality in concrete; while GnP is expected to enhance mechanical properties and microstructures along with developing piezoresistive self-sensing properties, SP is expected to enhance the internal curing, self-healing, and durability performance of concrete, specifically against the freeze-thaw condition.

For this investigation, the GnP used has been produced from a top-down method with slight altercations, as explained within the methodology section. The experiments conducted within the literature review embed GnPs and SP into mortar samples individually, but these admixtures will be combined with concrete for this investigation.

Evidence from the literature review clarifies that Sodium Polyacrylate particles should shrink during the hydration process, leaving voids in the concrete. Due to the atomic structure of the GnPs, they carry an electrical impulse/charge. Therefore, they should be able to sense nano cracks that occur alongside the voids and effectively seal up the cracks or potentially reduce void spaces over time. It should be noted that the voids left by the SP are crucial in aid of freeze and thaw resistance as voids in the concrete absorb the hydraulic pressure and provide additional space for the water to expand.

2. Materials and Method

2.1. Materials and concrete mix

Ordinary Portland Cement CEM I, 42.5R pure grade supplied by Dragon Alfa was used as the binder cement. Locally sourced river sand, and crushed granules were used as fine and coarse aggregates for each mixture. The sand used was graded with granules below 4mm in size. The coarse aggregate grade will be between 4mm and 10mm in diameter for the granules. Thermo-mechanically exfoliated GnP roughly 1-4 micrometre in diameter, comprised of ~10 layers and 2-3 μm in size, acquired from Zentek Ltd. in Canada and the SP, 300–700 µm in size acquired from Vibe-Nation in the UK was used.

The concrete mix design is presented in Table 2. The mixing ratio for cement, sand, coarse aggregate, and water is 1:2:3 (Rajput, 2020) without any additives. This will be used to compare against, a normal mix with 0.5g GnP per 1kg cement (GnP-C), a normal mix with 1g of SP per 1kg cement (SP-C) and a normal mix with both 0.5g of GnP and 1g of SP per 1kg of cement (GnP-SP-C). The GnP content was 0.05 wt% of cement which is in the range of optimum proportions according to the author's previous and other similar studies (Qureshi and Panesar, 2020, Wang et al. 2016, and Tao et al. 2019). Optimum proportions of SAP was taken 0.1 wt% of cement as similarly reported in Al-Nasra's (2013) to achieve maximum strength and durability performance. The water to cement ratio was kept constant in all mixes. This will help understand the synergic impact of GnP and SP on concrete.

Efficient dispersion of GnP and mixing of SP in concrete was one of the important steps in mixing. Firstly, for GnP-C and GnP-SP-C, 0.003kg of dry GnP powder was measured out twice using a fine-scale. Afterwards, this was mixed with 800ml of water in a glass beaker where a magnetic stirrer (500rmp) was used for 30 minutes and subsequently, placed in an ultrasonic bath for 10 minutes (Figure 1) then 5 minutes in a high shear mixer. This GnP is specifically treated to be dispersible in water. Then again the combination of magnetic stirring, ultrasonication and high share mixing process is simplified from Qureshi and Panesar (2020). Lastly, when mixing the GnP solution with the concrete in the drum mixer ensure to mix 85% of the solution at the beginning the afterwards, slowly, and sufficiently mix the rest in. Following that the preparation of SP for SP-C and GnP-SP-C is carried out by simply, measuring out 0.004kg of SP for SP-C and 0.005kg for GnP-SP-C separately. Then pour the dry mixtures into the dry cement and mix thoroughly for 5 minutes.

Concrete mixing was conducted following ASTM 192 (ASTM, 2019) procedure. Concrete cubes (100x100x100 mm) and prisms (100x100x300 mm) were prepared and cured in water until testing at 28 days (Figure 2). In addition to that, a wooden board was placed between two corners of the prisms to create a triangular prism shape. This was done to attain more sample specimens for testing without increasing control materials. Lastly, two 50x50mm copper sheets were embedded on the surface of samples GnP-C and GnP-SP-C, to measure the difference in piezoresistivity during the testing phase.

2.2. Methods

A Compressive Strength and Freeze-Thaw Test which all four groups will undergo and a Piezoresistive Strain Test which, only the samples with embedded copper GnP-C and GnP-SP-C will undergo have been designed to observe the changes in the properties of multifunctional concrete mixes. The microstructure investigation was carried out through a Scanning electron Microscope and Energy Dispersion X-Ray (SEM-EDX).

2.2.1. Compressive strength test

Concrete cubes after 28 days of curing were used for the test. The BS EN 12390-3:2019 has been used as a guideline to perform the compressive strength test using the Avery-Denison machine. Having cracked the samples, small fragments towards the epicentre of the cubes were broken off, placed in a universal glass bottle, and sent to the SEM-EDX lab, to attain images of the morphological structure.

2.2.2. Freeze-thaw test

The Freeze-Thaw test was conducted on eight prisms under a series of rapid temperature changes in a chlorinated environment. This to investigate concrete durability performance in a real-life case of coupled degradation mechanism, i.e., freeze-thaw under chloride attack. Triangular concrete prisms (100x100x300 mm) cured for 30 days prior to tasting. This specific sample arrangement was expected to have more impact area under harsh conditions allowing accurate chloride penetration depth measurement. Guidelines from the PD CEN/TS 12390-9:2016 – TC (BSOL, 2020), “Freeze-thaw Resistance with De-icing Salts” and ASTM C666/C666M-15 “Standard Test Method for Resistance of Concrete to Rapid Freezing and Thawing” (ASTM, 2015) has been simplified for this experiment due to time constraints. The freeze and thaw cycles were operated manually. The temperature of the concrete samples was measured using a digital thermometer coupling attached to the concrete samples throughout the whole freeze-thaw process. The prisms were placed in a freezer until they reached -18°. After reaching -18°, the samples were removed and de-iced each time with Sodium Chloride (salt) and manually placed in an oven to reach +4°. Once thawed, the samples were placed back in the freezer for the cycle to repeat ten times (two cycles per day as it took 2 hours to freeze and 1 hour to thaw). The freeze-thaw temperature change rate was maintained consistently, which is specific for this study and might affect the results if compared with a different rate of temperature change. Following the completion of 10 cycles, the samples were cracked using the compressive machine and sprayed with a silver nitrate solution to observe the chloride ion penetration through visual representation and the SEM-EDX.

The Silver Nitrate solution was made by mixing 4g of silver nitrate (RTF Chem; 99.9% Purity, CAS 7761-88-8, $AgNO_3$) with 250ml of cold distilled water. The Chloride will react with silver ions (Ag^+) to form an insoluble salt silver chloride (AgCl) (Equation 1). As a result, an exothermic result occurred as the surface of the specimen emitted heat. This method was adapted from Lo (2005).

Equation 1: Silver Nitrate and Chloride Equation.

$$Cl^- + AgNO_{3(aq)} \rightarrow AgCl_{(s)} + NO_3^-{}_{(aq)}$$

The solution was sprayed three times with an interval time of 30 minutes to ensure all parameters of the samples were coated with the solution. After leaving it for 24 hours the chloride ion penetration depth was apparent as the samples turned to purple colour. The chloride ions penetration predominantly occurred at the base of prisms. Therefore, the penetration depth was measured at least 5-10 places from the base of each prism cross-section surface, depending on the irregularity in samples. An average was taken for each type of concrete mix.

2.2.3. Microstructure investigation

From both the Compression and Freeze-Thaw test, cracked samples with an almost flat surface roughly 1/2 - 1cm in diameter were placed under an FEI Quanta 650 Field Emission Scanning Electron Microscope (SEM) and Energy Dispersive X-ray Microanalysis (EDX) with detection active area of 50mm^2 to obtain high-resolution images to observe for damages and changes from each test (Figure 5). Samples were submerged in acetone for an hour just after collection to inhibit further reactions. After acetone treatment samples were dried in a new universal bottle filled with silica gel for 1 hr, then placed in an oven at 50°C for 2hr. Finally, samples were attached to aluminium stubs using carbon tape, gold-coated using Emscope SC500 sputter coating unit: 28s, 10mA, 0.1Torr, - giving a nominal 10nm gold coat, and preserved in glass desiccator with silica gel for 2 hr prior to the SEM-EDX observation. The sample treatment process was simplified from Qureshi et al. (2016) to conduct the observation shortly after sample collection.

2.2.4 Piezoresistive response test

The Piezoresistive Strain Test was conducted following the ASTM C1760-12, and (ASTM, 2012) a 2-Electrode configuration (uniaxial method) made out of copper plates was embedded onto the 100x100mm cubes samples for GnP-C and GnP-SP-C to observe which sample conducts a better resistivity upon loading. The data obtained was carried out using the compressive testing machine as detailed in 2.2.1 and a BK Precision 891 multimeter with a data collection set up on a computer (Figure 1). The loading rate was 6KN/min, and cyclic loading was within the rage of 0 to 10 KN, i.e., much lower end of the elastic limit of concrete. This is to minimise the impact of plastic deformation or cracks that could have affect the results of electrical resistivity. In theory, as this is a uniaxial method, the distances of the conductive plates of a cement-based composite become closer from compression and enable an electrical current to flow. As compression increases, the GnP will be able to sense the pressure and thus observe a change in electrical resistivity. When unloading, the composite returns to its natural state and regains its initial electrical resistivity. The fractional change in resistivity ($\Delta R\%$) was measured using the following relation (Siahkouhi et al. 2021):

$$\Delta R\% = \left(\frac{R_L - R_0}{R_0}\right)$$

Here, R_0 is initial electrical resistivity (kΩ), and R_L is electrical resistivity during loading (kΩ).

3. Results and discussion

3.1. Compressive strength

The compressive strength of concrete mixes is presented in Figure 2. GnP containing concrete mixes shows higher compressive strength in GnP-C and GnP-SP-C, resulting in about 14% and 6% enhancement, respectively, compared to the control mix. Enhancement of mechanical strength of concrete by GnP is possibly due to increasing hydration mechanism, nano-core effect and reinforcing effect at a nano-microstructural level of the concrete matrix. Other studies also reported similar evidence: cement hydration accelerated by GnPs with the enhancement of the polymerisation degree of calcium silicate hydrate (C-S-H) (Wang et al. 2019, Qureshi and Panesar 2020), the nano-core effect due to the ultra-high specific surface area resulted in the deposition of hydration production on the nano fillers (Han et al., 2017[b]), the conversion of pore water inside C–S–H gel causing a reorganisation of gel structure (Wang et al. 2021), and pore filling and bonding effect (Han et al., 2017b, Qureshi and Panesar 2020). SP on the other hand, decreases the compressive strength of SP-C by about 9%, compared to the control mix. Although SP was expected to enhance the mechanical properties to some extent, the strength may be impacted by the higher proportions of larger size (over 500 µm) SP in the mix. As noted by Al-Nasra (2013) "Excess amount of SP creates larger voids within the concrete, which results in a weaker concrete in terms of both strength and durability". The combined impact of SP and GnP eventually resulted in slightly enhanced compressive strength in GnP-SP-C compared to the control mix, which is reasonable.

3.2. Freeze-thaw response

Strong structural integrity with little to no cracks occurring on the surface was evident prior to initiating the freeze-thaw cycle. Figure 3 depicts concrete sample surface images during freeze-thaw cycles. After removing the samples from the freezer, salt was applied to de-ice the sample and reduce the number of freezing and thawing cycle exposures to the samples by significantly lowering the freezing point. This enables coupled degradation mechanism resulting in more frequent and damaging cycles to be undergone.

Through visual diagnosis from Figure 3, damages started occurring after the 2nd cycle and hereby fine cracks either slowly increased in diameter and depth or new smaller indents and holes became apparent. All samples displayed spalling and scaling on the surface due to water expansion and sodium chloride penetration. Also, all samples exposed uncracked aggregates and gaps around the aggregates. However, with the GnP-SP-C, these types of cracks were not as apparent as shrinkage did not occur, meaning that moisture was not lost, which dries out concrete.

Surface parallel cracking towards the 8th cycle was identified in all the samples due to the large build-up of water ions, causing the concrete to internally expand due to the stress of not being able to contain the water ions. Towards the end of the 9th and 10th cycles, medium/large chunks of the edges of the samples are breaking apart in the control mix and GnP-C due to not having enough space allowing ice volume expansion within the concrete matrix.

The SP-C and GnP-C presented fewer surface cracks and gaps at the end of 10 cycles. This corroborates with the findings from Daoud and Al-Nasra (2014), in the sense that the SP acts as air entrainment and, when uniformly distributed, leaves larger pores once shrunk. As this occurs, the GnP would maintain the integrity of the concrete or potentially reduce the air void space by sealing cracks that may occur due to its multiple layers of sheets.

The cracked surface of prisms after the freeze-thaw test was spared with silver nitrate solution, which produced distinct pink to purple colour clearing the boundary of chloride depth penetration. Figure 4 presents images of the cracked surface following silver nitrate spray. Photographic evidence suggests that chloride ions did not fully penetrate the samples from all directions, and the majority occurred towards the prism's base. Therefore, representing chloride penetration depth were measured from the base of the prisms for comparisons, as presented in Figure 5. The control mix exhibited greater chloride ion penetration compared to the other samples. This indicates high porosity within the control concrete specimen, meaning that permeability was greater, allowing chloride ion ingress. The control mix showed signs of shrinkage very early during the freeze-thaw cycle displaying minor gaps and cracks. Due to water expansion on the holes from freezing and thawing, the gap increased or new ones were produced, allowing greater penetration. GnP and SP individually decreased 11% and 22 % depth of chloride penetration, respectively, compared to the control mix. This indicates SP individually results in better durability performance in concrete under freeze-thaw and chloride ingress than GnP in the concrete mix.

In comparison, the GnP-SP-C displayed better durability in preventing chloride ion ingress under freeze-thaw conditions, resulting 42% decrease in the depth of chloride penetration compared to the control mix. This could be due to the combined effect of GnP and SP on the concrete matrix. However, it could be argued that as the samples were manually de-iced, the same level of de-icing salt may not have been applied to all samples.

3.3 Microstructure of concrete

Microstructural observation of concrete mixes was conducted using SEM-EDX before and after the freeze-thaw experiment. Microstructural SME image and EDX element semi-quantification of concrete mixes prior to the freeze-thaw test are presented in Figures 6a and b (control), c and d (GnP-C), e and f (SP-C), g and h (GnP-SP-C). The morphological characteristics of the different samples can be observed with similar EDX elemental quantification patterns in all mixes confirming common hydration products, such as C-S-H, portlandite and ettringite. Figures 6c indicate that the GnP sheets were dispersed efficiently and compacted well within the cement matrix. Figure 6e depicts the bonding between the SP molecules and an even dispersal of SP along the surface of the sample with some SP swelling more than others. Much larger sizes of SP were noted in other SEM images. However, the GnP seem to have encapsulated itself in the holes of the concrete to fill in the gap and strengthen the specimen. This is similarly reported in Han et al. (2017[b]) and Qureshi and Panesar (2020). Figure 6g shows the SP partly covering the surface of the GnP samples whilst the GnP are encapsulated in the porous zone of concrete matrix. This could indicate the sealing of micro-cracks that may have started occurring due to the follicle style strands branching out, attaching to the GnP and SP, which increase the strength and durability performance of the concrete matrix.

Freeze-thaw depicts morphological changes to the concrete microstructure as presented in Figures 7a and b (control), c and d (GnP-C), e and f (SP-C), g and h (GnP-SP-C). Firstly, figure 7a displays a few microcracks occurring and silver chloride dispersed on the surface. Gaps were also visible in the sample where water had been entrapped and expanded during the freezing cycle to crack the sample. This validates Figures 4 and 5 findings, resulting in a higher chloride ion penetration depth in the control concrete mix. Figure 7c shows overlapping layers for GnP and triggering of secondary hydration products formation such as C-S-H and Ettringite morphologies which may have retracted the cracks due to freeze-thaw as well as further permeation of chloride ions. The elemental composition in the EDX (Figure 7d) also shows C-S-H, calcium hydroxide and Ettringite formation indication. Figure 7e presents SP with some penetrating gaps present in the SP-C sample, which the SP is not enveloping. This could be due to the size of SP. The SP is not fully apparent in Figure 7g, suggesting that it may be encapsulated underneath the GnP and secondary cement hydration products, protecting the sample as the silver chloride is dispersed on top of the GnP as opposed to minor particles on the cement paste. This does substantiate Figures 4 and 5 as it indicates higher durability due to low porosity and permeability, reducing penetration. Also, the follicle strand types in GnP-C and GnP-SP-C concrete after freeze-thaw (Figures 7c and g) are greater than the state of concrete before freeze-thaw (Figures 6c and g), indicating that the sample may be trying to seal itself after the damage occurring in freeze-thaw cycles. This resembles Snoeck et al. (2012) reported self-healing performance of SP containing concrete.

3.4 Piezo-resistive performance of self-sensing of concrete with GnP

Figure 8 presents the response of fractional change in electrical resistivity to compressive stress as an indicator of the self-sensing performance of concrete with GnP. The fractional change in electrical resistivity shows stable consistency to the compressive stress in both GnP-C and GnP-SP-C (Figure 8a). The response was similar in all three cycles of loading with time (Figure 8b). The amplitude of changes in the electrical resistivity in GnP-C increased by 2% compared to GnP-SP-C, which indicates higher sensing ability. This may be owing to the SP inclusion in the concrete mix, which creates voids and slightly decreases the piezo-resistive network in the composite matrix. Considering the cross-section of the cube samples (100x100mm), the fractional change in resistivity varied up to 12.7%/MPa in GnP-C concrete, which is reasonable sensing considering the lower dosage of GnP (0.05 wt% cement) and stress level 1MPa during cyclic loading. However, the fractional change in resistivity of a self-sensing cement-based composite can reach up to 70% with a higher dosage of a CNT-cement hybrid in the PC based cement composite (25 wt% in PC) at a stress level of 12.5 MPa (Ding et al. 2022).

3.5 Multifunctionality

Both the GnP and SP have a respective impact on the concrete matrix, and their combination results in a synergetic effect. Through testing and analysis, the self-sealing capabilities of the modified concrete were investigated, and it was found that GnP-SP-C, over time, enhanced the capabilities of concrete. The self-sensing abilities of the composite also increased by GnP into the matrix. The study on the impact of GnP and SP on the microstructure of the concrete matrix did indicate in a few specimens of a self-sealing process which could be an indication that the admixtures sensed the damage in the sample and enveloped into the gaps to heal/seal itself. The self-sealing/healing ability of SP is previously reported in the literature (Qureshi and Abir, 2020), and its combination with GnP shows increasing performance potential. However, this is open to interpretation as much more experimenting is required to prove this.

The experimental findings suggest the prospects for multifunctionality in GnP-SP-C mix compared to other concrete mixes. Figure 9 presents a comparative prospect for different concrete mixes under different service functions: mechanical strength, durability, service life, smart function, and cost-effectiveness. The performance is categorised 1 to 4, 1 being the lowest performance/service potential and 4 being the highest performance/service potential. Typical concrete, herein the control mix, is the most cost-effective when other functionalities are limited. A small proportion of GnP and SP makes GnP-C and SP-C more functional. GnP-C shows enhancement in strength, durability, and self-sensing smart functionalities. SP-C shows enhancement in durability, particularly against chloride attack under freeze-thaw coupled degradation mechanism, as well as the self-healing smart properties. Hence, the combination of both of those in GnP-SP-C shows a synergetic effect resulting in a balanced enhancement in mechanical strength property, superior performance enhancement in durability performance and smart properties, potentially both self-healing and self-sensing performance.

Nevertheless, the existing study has limitations in terms of a broader range of mix design and experimentation with other aspects of concrete functionality and microstructural understanding. GnP-SP-C shows prospects for multifunctional concrete, although further comprehensive experiment is required to determine the percolation threshold of GnP and optimise the proportions of SP in the concrete mix. Also, an extensive experimental scheme will be undertaken to study the kinetic properties, GnP-cement, SP-cement and GnP-SP microstructural interaction, and other functionalities of such advanced concrete.

5. Conclusions

This project aimed to disperse Graphene Nanoplatelets (GnP) with Sodium Polyacrylate (SP) in concrete to observe the changes in mechanical properties through a range of experimental tests and determine whether or not these additives can seal and/or sense the concrete when damaged. Having undertaken the experiments, results suggested that GnP with SP embedded into concrete does provide a stronger, durable, i.e., freeze-thaw and chloride ion penetration resistant, and self-sensing materials. GnP enhanced the strength, conductivity, and durability performance of concrete, while SP slightly decreased strength, then again enhanced concrete's self-healing and durability performance. The combination of GnP and SP shows a synergetic impact on the GnP-SP-C concrete mix, which developed multifunctional serviceability in concrete. The GnP-SP-C shows examples of its sealing and piezoresistive sensing capabilities as verified by microstructural and electrical resistivity analysis of the samples. Although the GnP-SP-C specimen was a 6% more compressive strength than the control concrete mix, with the internal curing from the SP, the specimen would likely increase gradually in strength as time proceeds, thus anticipating a higher compressive strength than the original one experimented. Furthermore, it should be noted that the GnP and SP from Freeze-Thaw seem to overlap and agglomerate on one another, providing protective support on the surface of the concrete to help maintain the structure's integrity in the long run.

The self-sensing aspect of this project acts as a catalyst for further research to be undertaken with creating improved multifunctional concrete which allows piezoresistivity strain/stress to be measured and be applied in real-life construction applications to structural health monitoring. This project could pave the way for a new innovative idea in creating long-lasting, low-maintenance, smart and sustainable concrete.

Acknowledgement

The authors are grateful for Tanvir Qureshi's Vice-Chancellor Early Career Research (VCECR) grant award and the IFA: New Starters (Faculty funded) award by the University of the West of England, Bristol, UK. The authors are also grateful for the graphene materials supply and collaboration with Zentec Ltd., Canada.

Data Availability Statement

Some or all data, models, or code that support the findings of this study are available from the corresponding author upon reasonable request.

References

Al-Nasra, M. (2013) Optimising the Use of Sodium Polyacrylate in Plain Concrete. *International Journal of Engineering Research and Applications (IJERA)* [online]. 3(3), pp.1058-1062.

Anandkumar, M., Suriya, M. and Ravichandran, P. (2020) Experimental Study on Effect of Super Absorption Polymers in Surface Cracked Concrete Structures. *International Journal of Scientific & Technology Research* [online]. 9(2), pp.812-815.

ASTM. (2012) Standard Test Method for Bulk Electrical Conductivity of Hardened Concrete [online] *ASTM International*, West Conshohocken, PA.

ASTM. (2015) Standard Test Method for Resistance of Concrete to Rapid Freezing and Thawing [online]. *ASTM International*, West Conshohocken, Pa.

ASTM. (2019) Standard Practice for Making and Curing Concrete Test Specimens in the Laboratory *ASTM International* [online], West Conshohocken, PA.

British Standards, 2002. *Testing hardened concrete. Part 3: Compressive strength of test specimens. BS EN 12390-3,* s.l.: s.n.

Chen, G., Yang, M., Xu, L., Zhang, Y. and Wang, Y. (2019) Graphene Nanoplatelets Impact on Concrete in Improving Freeze-Thaw Resistance. *Applied Sciences* [online]. 9(17), p.35.

Daoud, M. and Al-Nasra, M. (2014) The Use of Super Absorbent Polymer as a Sealing Agent in Plain Concrete. *American Journal of Engineering Research (AJER)* [online]. 3(3), pp.132-137.

Ding, H., Zhang, L. and Zhang, P. (2017) Factors Influencing Strength of Super Absorbent Polymer (SAP) Concrete. *Transactions of Tianjin University* [online]. 23(3), pp.245-257.

Ding, S., Xiang, Y., Ni, Y. Q., Thakur, V. K., Wang, X., Han, B., & Ou, J. (2022). In-situ synthesising carbon nanotubes on cement to develop self-sensing cementitious composites for smart high-speed rail infrastructures. Nano Today, 43, 101438.

Dong, W., Li, W., Tao, Z. and Wang, K. (2019) Piezoresistive properties of cement-based sensors: Review and perspective. *Construction and Building Materials* [online]. 203, pp.146-163.

Han, B., Zheng, Q., Sun, S., Dong, S., Zhang, L., Yu, X., & Ou, J. (2017). Enhancing mechanisms of multi-layer graphenes to cementitious composites. Composites Part A: Applied Science and Manufacturing, 101, pp. 143-150.

Han, B., Zhang, L., Zeng, S., Dong, S., Yu, X., Yang, R., & Ou, J. (2017). Nano-core effect in nano-engineered cementitious composites. Composites Part A: Applied Science and Manufacturing, 95, 100-109.

Han, B., Ding, S., Wang, J., & Ou, J. (2019). Basic principles of nano-engineered cementitious composites. In Nano-Engineered Cementitious Composites, Springer, Singapore, pp. 1-96.

Jensen, M. (2013) Use of superabsorbent polymers in concrete. *Concrete International* [online]. 35(1), pp.48-52.

Jensen, O. and Hansen, P. (2001) Autogenous deformation and RH-change in perspective. *Cement and Concrete Research* [online]. 31(12), pp.1859-1865.

Kevern, J. and Farney, C. (2012) Reducing curing requirements for pervious concrete using a superabsorbent polymer for internal curing. *Transportation Research Record* [online]. 2290, pp. 115–121.

Le, J., Du, H. and Pang, S. (2014) Use of 2D Graphene Nanoplatelets (GNP) in cement composites for structural health evaluation. *Composites Part B: Engineering* [online]. 67, pp.555-563.

Lee, S., Ha, K., Jung, Y., Jang, S. and Yeo, I. (2014) Characteristics of mortar containing sodium polyacrylate absorbent synthesised by inverse emulsion polymerisation. *KSCE Journal of Civil Engineering* [online]. 18(5), pp.1397-1402

Lo, T. (2005) Carbonation & Chloride Penetration of Concrete Structures, City University of Hong Kong

Long, W., Wei, J., Xing, F. and Khayat, K. (2018) Enhanced dynamic mechanical properties of cement paste modified with graphene oxide nanosheets and its reinforcing mechanism. *Cement and Concrete Composites* [online]. 93, pp.127-139.

Long, W., Ye, T., Li, L. and Feng, G. (2019) Electrochemical Characterization and Inhibiting Mechanism on Calcium Leaching of Graphene Oxide Reinforced Cement Composites. *Nanomaterials* [online]. 9(2), pp.2-19.

Manzur, T., Iffat, S. and Noor, M. (2015) Efficiency of Sodium Polyacrylate to Improve Durability of Concrete under Adverse Curing Condition. *Advances in Materials Science and Engineering* [online]. pp.1-8.

Mohammed, A., Sanjayan, J., Duan, W. and Nazari, A. (2016) Graphene Oxide Impact on Hardened Cement Expressed in Enhanced Freeze-Thaw Resistance. *Journal of Materials in Civil Engineering* [online]. 28(9), pp.1-6.

Olafusi, O., Sadiku, E., Snyman, J., Ndambuki, J. and Kupolati, W. (2019) Application of nanotechnology in concrete and supplementary cementitious materials: a review for sustainable construction. *SN Applied Sciences* [online]. 1(6), pp.1-8.

Qureshi, T. and Al-Tabbaa, A. (2020) Self-Healing Concrete and Cementitious Materials. *Advanced Functional Materials*.

Qureshi, T. S. and Panesar, D. K. (2017) A review: the effect of graphene oxide on the properties of cement-based composites, *CSCE Annual Conference*. Vancouver, Canada, pp. 642-1 to 642-10.

Qureshi, T. S. and Panesar, D. K. (2019) A comparison of graphene oxide, reduced graphene oxide and pure graphene: early age properties of cement composites. *2nd RILEM Spring Convention & International Conference on Sustainable Materials, Systems and Structures*. [online].

Qureshi, T. S. and Panesar, D. K. (2019) Impact of graphene oxide and highly reduced graphene oxide on cement-based composites. *Construction and Building Materials* [online]. 206, pp. 71–83.

Qureshi, T. S. and Panesar, D. K. (2020) Nano reinforced cement paste composite with functionalised graphene and pristine graphene nanoplatelets. *Composites Part B: Engineering*. 197, p. 108063.

Qureshi, T., Panesar, D., Sidhureddy, B., Chen, A. and Wood, P. (2019) Nano-cement composite with graphene oxide produced from epigenetic graphite deposit. *Composites Part B: Engineering*, 159, pp.248-258.

Qureshi, T. S., Panesar, D. K. and Peterson, K. (2019) Thin section microscopy and DVS study to determine the influence of graphene materials on the microstructure of cement-based composite. *17th Euroseminar on Microscopy Applied to Building Materials* [online]. pp. 134–140.

Qureshi, T., Kanellopoulos, A. and Al-Tabbaa, A. (2016) Encapsulation of expansive powder minerals within a concentric glass capsule system for self-healing concrete. *Construction and Building Materials* [online]. 121, pp.629-643.

Rajput, K. (2020) Concrete Mix Ratio | What Is Concrete Mix Ratio | Types of Concrete Mix Ratio. Available from: https://civiljungle.com/concrete-mix-ratio/

Siahkouhi, M., Razaqpur, G., Hoult, N., Hajmohammadian Baghban, M. and Jing, G. (2021) Utilisation of carbon nanotubes (CNTs) in concrete for structural health monitoring (SHM) purposes: A review. *Construction and Building Materials*, 309, pp.125-137.

Snoeck, D., Van Tittelboom, K., De Belie, N., Steuperaert, S. and Peter Delruel, P. (2012) The Use of Superabsorbent Polymers as a Crack Sealing and Crack Healing Mechanism in Cementitious Materials. 3rd International Conference on Concrete Repair, Rehabilitation and Retrofitting [online]. pp. 152 – 157.

Sun, S., Han, B., Jiang, S., Yu, X., Wang, Y., Li, H., & Ou, J. (2017). Nano graphite platelets-enabled piezoresistive cementitious composites for structural health monitoring. Construction and Building Materials, 136, pp. 314-328.

Tao, J., Wang, X., Wang, Z. and Zeng, Q. (2019) Graphene nanoplatelets as an effective additive to tune the microstructures and piezoresistive properties of cement-based composites. Construction and Building Materials [online]. 209, pp.665-678.

Wang, B., Jiang, R. and Wu, Z. (2016) Investigation of the Mechanical Properties and Microstructure of Graphene Nanoplatelet-Cement Composite. Nanomaterials [online]. 6(11), p.200.

Wang, J., Han, B., Li, Z., Yu, X., & Dong, X. (2019). Effect investigation of nanofillers on CSH gel structure with Si NMR. Journal of Materials in Civil Engineering, 31(1), 04018352.

Wang, J., Dong, S., Zhou, C., Ashour, A., & Han, B. (2021). Investigating pore structure of nano-engineered concrete with low-field nuclear magnetic resonance. Journal of Materials Science, 56(1), 243-259.

Wu, S., Qureshi, T. and Wang, G., 2021. Application of Graphene in Fiber-Reinforced Cementitious Composites: A Review. *Energies*, 14(15), p.4614.

Tables

Table 1. Property changes in concrete with the addition of Nanoparticles

Property changes	**Outcomes**
Mechanical and Electrochemical Properties	Increased Strength, Ductility, Electrical Conductivity, Corrosion Inhibition and Reduced Water Permeability
Concrete Durability	Watertightness and reduced shrinkage eliminate the number of joints required and minimise curling and warping by reducing concrete's change in volume from temperature changes and loss of moisture
Surface protection of the reinforcement through applications of surface coatings	Nano modified reinforcement for concrete in a corrosive environment
Long-term maintenance and monitoring	Search and detect moisture presence, temperature, stress strain, and cracking.
Bulk Property	Help obtain thinner structural element, faster setting time, lower levels of environmental attack
Environmental Stability	Use marginal and recycled materials to make nanomaterials.

Table 2. Concrete mixes were used for this study.

Concrete mix	PC (Kg)	Water (Kg)	FA (Kg)	CA (Kg)	GnP (Kg)	SAP (Kg)	Total (Kg)
Control	4.200	2.800	7.650	10.550	--	--	25.200
GnP-C	5.040	3.360	9.180	12.660	0.003	--	30.243
SP-C	4.200	2.800	7.650	10.550	--	0.004	25.204
GnP-SP-C	5.040	3.360	9.180	12.660	0.003	0.005	30.248

Figure Captions

Figure 1. Typical sample setup for electrical resistivity response measurement under cyclic compressive stress.

Figure 2. Compressive strength of concrete mixes.

Figure 3. Images of the concrete surface after freeze-thaw cycles (not in scale).

Figure 4. Image of chloride depth penetration in concrete samples crack surface after AgNO3 application.

Figure 5. Depth of chloride penetration in concrete mixes.

Figure 6. Typical SEM images and EDX quantification of gross area of concrete before freeze-thaw, (a) Control (b) EDX from control, (c) GnP-C, (d) EDX from GnP-C, (e) SP-C, (f) EDX of SP-C, (g) GnP-SP-C, and (h) EDX of GnP-SP-C.

Figure 7. Typical SEM images and EDX quantification of gross area of concrete after freeze-thaw, (a) Control (b) EDX from control, (c) GnP-C, (d) EDX from GnP-C, (e) SP-C, (f) EDX of SP-C, (g) GnP-SP-C, and (h) EDX of GnP-SP-C.

Figure 8. Piezo-resistive performance of concrete for self-sensing, (a) fractional change in resistivity response against loading, and (b) fractional change in resistivity response under three cyclic loading (0.1 KN/sec).

Figure 9. A comparison of multifunctionality in different concrete mixes (1 being the low ranking and 4 being the high ranking).

Figure 1. Typical sample setup for electrical resistivity response measurement under compressive stress.

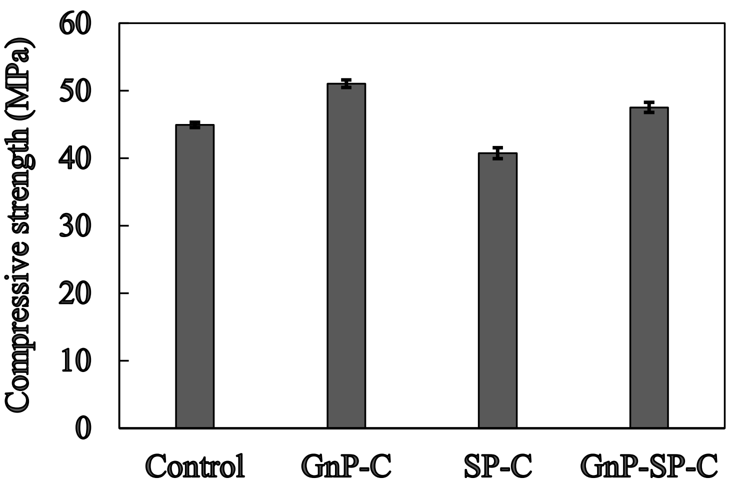

Figure 2. Compressive strength of concrete mixes.

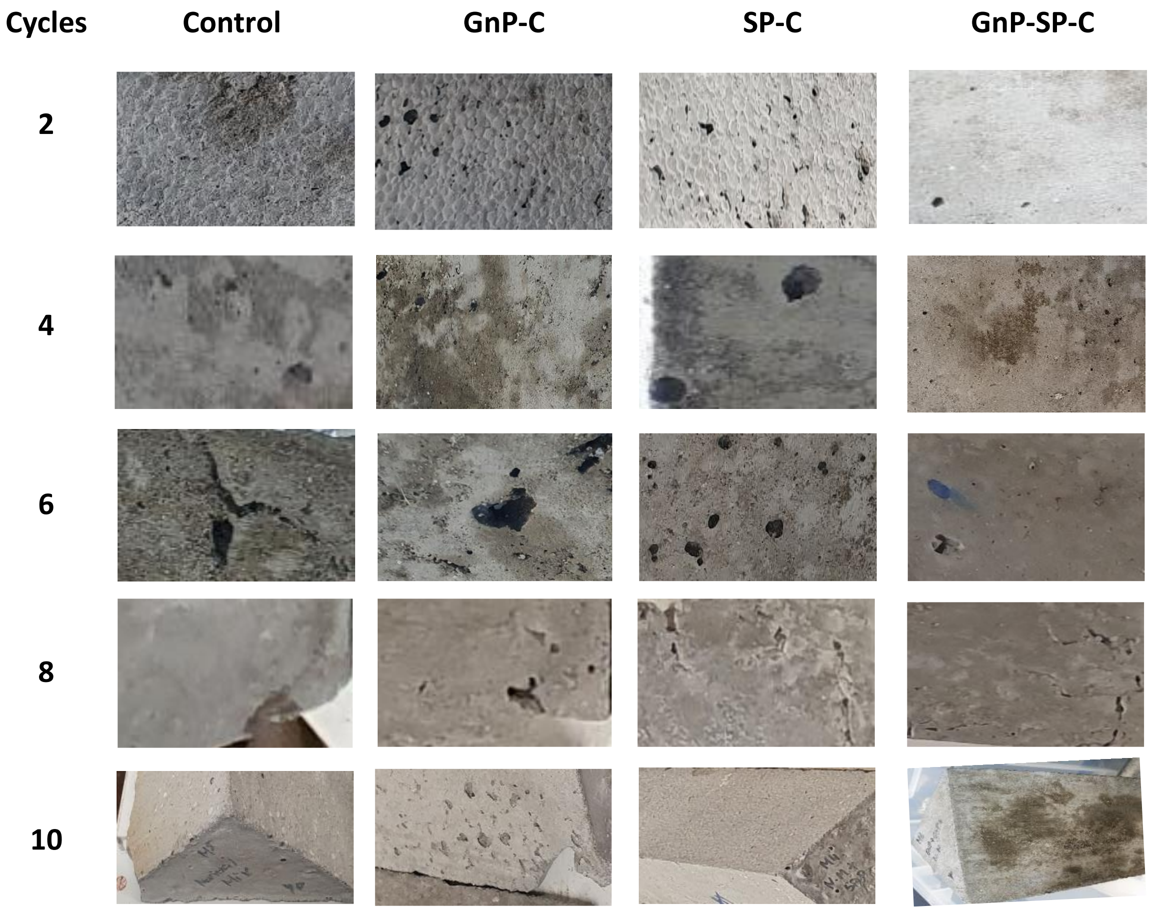

Figure 3. Images of the concrete surface after freeze-thaw cycles (not in scale).

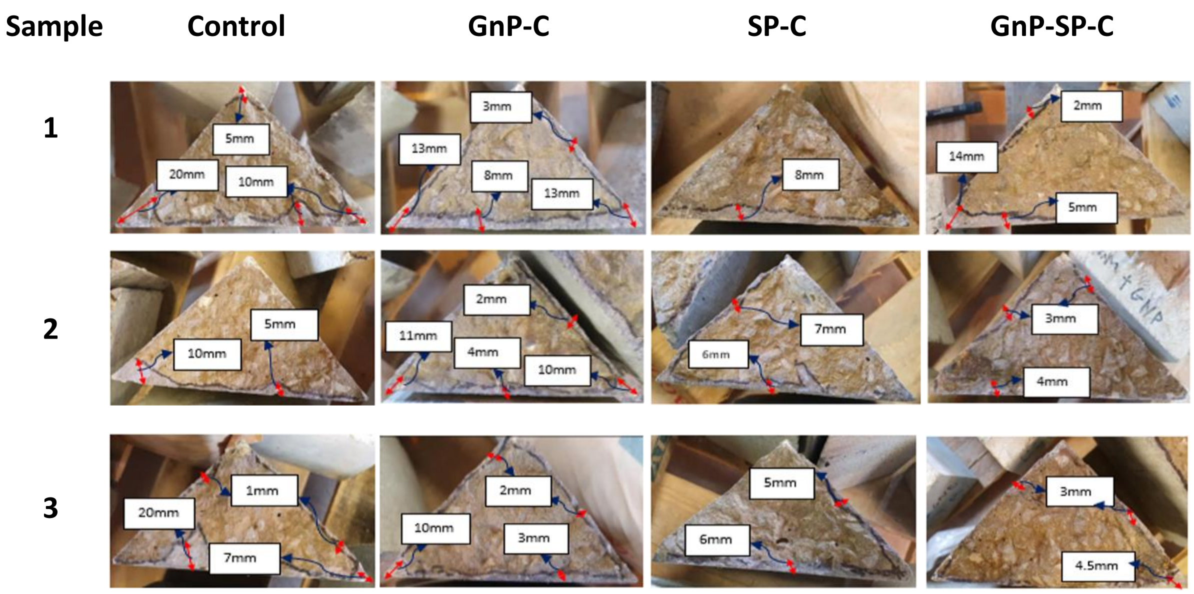

Figure 4. Image of chloride depth penetration in concrete samples crack surface after AgNO3 application.

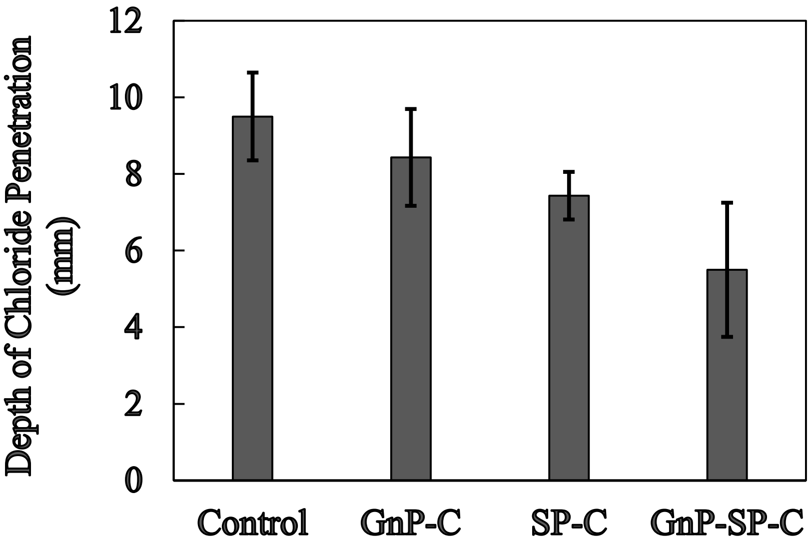

Figure 5. Depth of chloride penetration in concrete mixes.

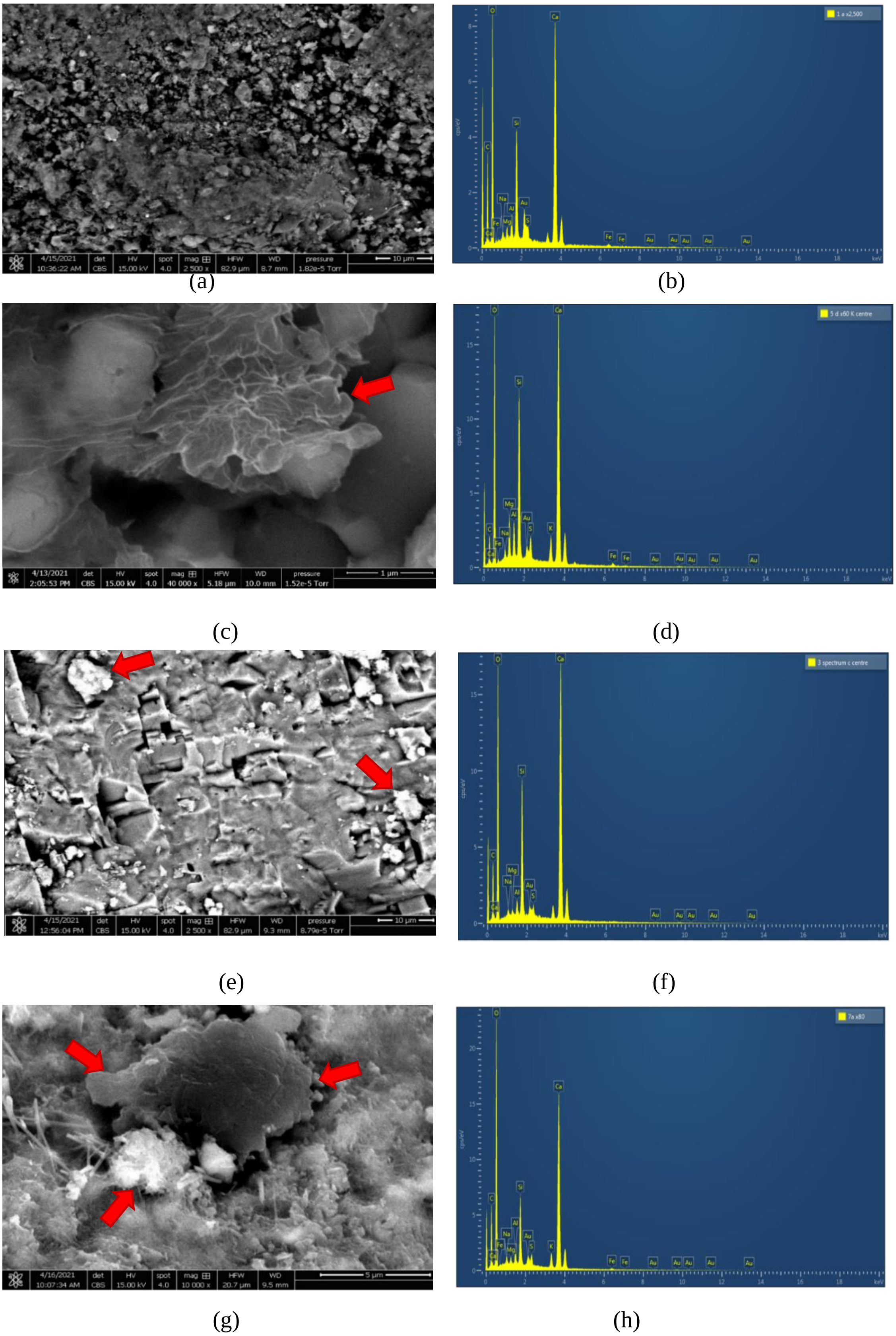

Figure 6. Typical SEM images and EDX quantification of gross area of concrete before freeze-thaw, (a) Control (b) EDX from control, (c) GnP-C, (d) EDX from GnP-C, (e) SP-C, (f) EDX of SP-C, (g) GnP-SP-C, and (h) EDX of GnP-SP-C.

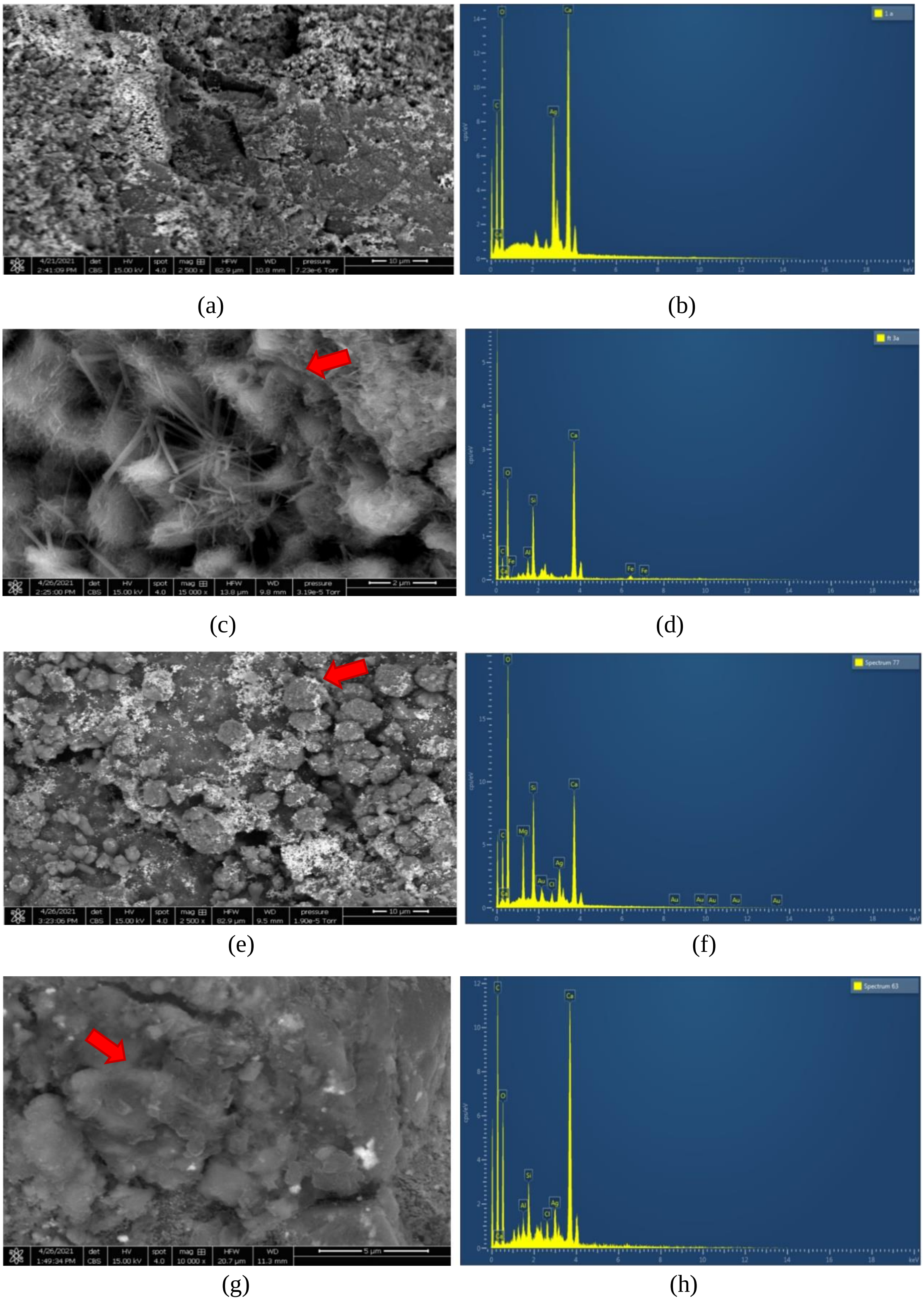

Figure 7. Typical SEM images and EDX quantification of gross area of concrete after freeze-thaw, (a) Control (b) EDX from control, (c) GnP-C, (d) EDX from GnP-C, (e) SP-C, (f) EDX of SP-C, (g) GnP-SP-C, and (h) EDX of GnP-SP-C.

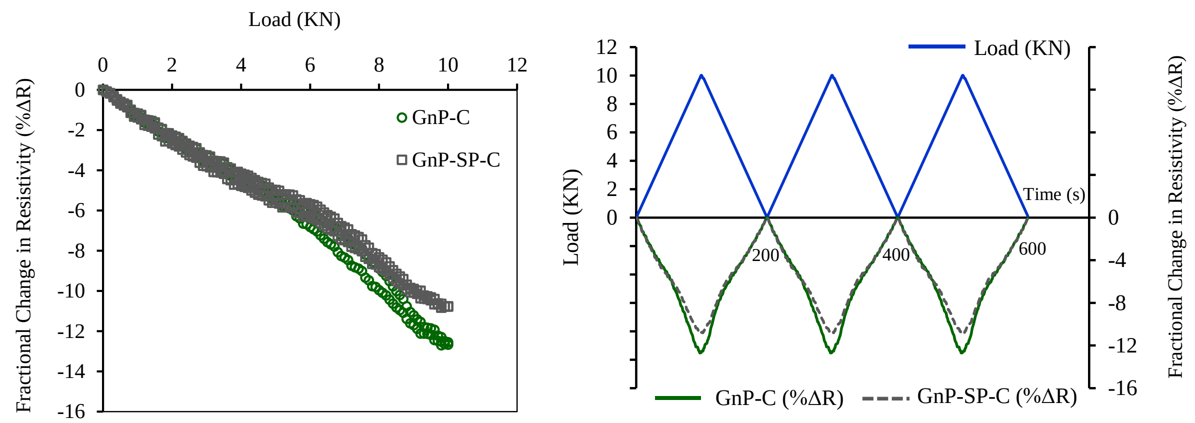

(a) (b)

Figure 8. Piezo-resistive performance of concrete for self-sensing, (a) fractional change in resistivity response against loading, and (b) fractional change in resistivity response under three cyclic loading (0.1 KN/sec).

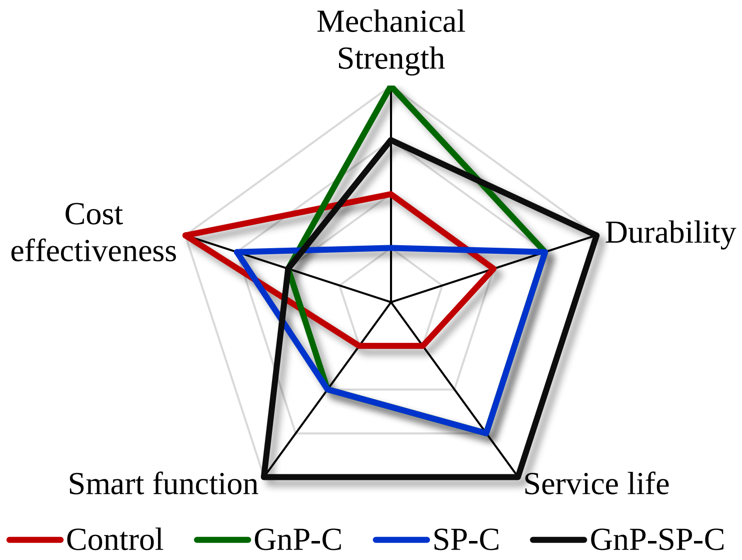

Figure 9. A comparison for multifunctionality in different concrete mixes (1 being the low ranking and 4 being the high ranking).